JOURNAL OF DYNAMICS AND CONTROL

VOLUME 8 ISSUE 9

# DESIGN AND ANALYSIS OF DEFECTED GROUND STRUCTURES INTEGRATED INSET FEED MICRO-STRIP PATCH ANTENNA AT 5.9GHZ FOR WI-FI BAND APPLICATIONS

Sanjeev Thapa[1], Surendra Shrestha[2], Ram Krishna Maharjan[3]

[1]Faculty of Science and Technology, School of Engineering, Pokhara University, Kaski - 33700, Nepal

[2,3]Department of Electronics and Computer Engineering, Institute of Engineering, Tribhuvan University, Lalitpur- 284403, Nepal

# DESIGN AND ANALYSIS OF DEFECTED GROUND STRUCTURES INTEGRATED INSET FEED MICRO-STRIP PATCH ANTENNA AT 5.9GHZ FOR WI-FI BAND APPLICATIONS

**Sanjeev Thapa[1*], Surendra Shrestha[2], Ram Krishna Maharjan[3]**

*[1]Faculty of Science and Technology, School of Engineering, Pokhara University, Kaski - 33700, Nepal*
*[2,3]Department of Electronics and Computer Engineering, Institute of Engineering, Tribhuvan University, Lalitpur- 284403, Nepal*

**[*]Corresponding Author: sanjeev5775thapa@gmail.com**

*ABSTRACT: This paper aims to design an optimized inset feed MPA for Wi-Fi band applications to resonate at 5.9 GHz. Defected ground structures (DGS) in dumbbell (DB) shape and Slot were etched to maximize the device's performance; the impedance of the antenna was perfectly matched with the impedance of the micro-strip line at 50 Ω. Improved bandwidth was achieved compared to the state-of-the-art MPA reported. The design methodology of the proposed antenna proceeds with a simulation of conventionally computed inset feed MPA using Ansys HFSS. The rectangular slot and DB-shaped DGS were etched on the ground plane at the same positions. Their effects on the performances of the antenna are comparatively analyzed by varying the dimensions. Further, the conventional, optimized, and antenna integrated with DB-shaped and slot-type DGS were analyzed with a fabricated prototype built in the laboratory. The performances of the prototype of the proposed antenna were found to be in good agreement with the simulated one. The defects in the ground plane are utilized to reduce the resonating frequency, bandwidth was upgraded to 300 MHz, a gain of 4.7 dB was achieved at a minimum measured return loss of -33.16 dB and back lobes were reduced.*

*KEYWORDS: Bandwidth, Defected Ground Structure, Dumbbell, Micro-Strip Antenna, RF Energy, Wi-Fi Band*

## 1. INTRODUCTION

Wi-Fi band is an ambient source of radio frequency (RF) energy available everywhere unlicensed. One of the most necessary units required to reuse such ubiquitous energy to power the distributed electrical devices and the Internet of Things (IoT), is to design an electromagnetic (EM) receiving module to support the Wi-Fi range of frequencies. Micro-strip patch antenna (MPA) is common in practice to use in wireless communication. Wi-Fi is now a commonplace technology in both indoor and outdoor settings, offering a plentiful supply of RF energy that is always present. It would be ideal if some receiving devices could utilize somehow wasted energy at 2.4 GHz and 5.9 GHz Wi-Fi radiation [1], either transforming directly into electrical energy to immediately power low-power electronic circuits or storing it for future use [2],[3]. The primary approach for utilizing the ambient RF energy is to have an efficient receiving module, with significant operating bandwidth and sufficient gain [4].

Due to the increased use of portable wireless devices, wireless frequency bands have become a key problem in communication systems [5,6], making it difficult to miniaturize the aerial while maintaining high performance throughout the bands. Practically in all wireless applications, micro-strip antennas are chosen. Because of its numerous benefits, including conformal design, compatibility with integrated circuits, low weight, low volume, and cheap cost, the micro-strip patch antenna (MPA) has proven to be an effective radiator for many applications [7]. Narrow bandwidth, low efficiency, high Ohm loss, ability to withstand low RF power, and low gain are the drawbacks of MPA. The performance of the MPA has been improved by utilizing a variety of methods. A commonly used technique is a defective ground structure (DGS) [4], which is used a lot in modern active and passive devices. Depending on

its geometry and size, each DGS shape has characteristics that influence the device's performance [8], [9]. Like minimizing component size, boost operational bandwidth and gain, decrease the mutual coupling between two networks, suppress higher-order harmonics, and avoid unwanted cross-polarization [5]. So, DGS has been etched to improve the performance of the antenna.

The literature regarding MPA design for wireless communication has reported maximum use of the operating frequency at S-band and 5G bands; although their bandwidth performances were poor, they have large sizes and complex design structures. In paper [10], the proposed patch antenna, operating at 28 GHz, has a complex design structure, although it presents improved bandwidth. Similarly, the MPA designed in [6-8], operates at 2.5 GHz, even after integrating DGS, reporting a bandwidth of 64.23 MHz and 67 MHz only; in addition, no miniaturization is achieved. An Inset-feed MPA are the most widely implemented antennas for numerous radio applications due to their simple geometry and excellent performance. For example, wireless LAN applications, GPS, and radar use inset feeding techniques [6]. The 5.9 GHz frequency is virtually not in use; instead, this range could address the high demand for RF spectrum required to connect the increasing numbers of devices, which could result in drastic economic benefits for the country too. The 5.9 GHz band could be the better option to provide the fastest GB range data connectivity at minimum cost to the public. Recently, researchers have become interested in the efficient harvesting of such an always-on ambient source of energy and its potential to power the electrically distributed systems in the future. Virtually unused 5.9 GHz frequency can fulfill the increasing market demand for RF spectrum and could contribute to the economic benefits of providing super-fast connectivity.

Design of MPA operating at Wi-Fi band 5.9GHz for receiving the freely radiating energy in the surrounding space and utilizing it to power the distributed electronic devices is

the major scope of this research [11]. This allows a versatile receiver unit to harvesting the freely available RF energy. The state-of-art in antenna design insights the 5.9GHz band of frequency is not in preference of researchers. So, researcher decides on designing and optimizing a receiving MPA for application in harvesting RF energy being wasted at 5.9GHz band and at the mean time exploring the effects of DB-shaped and rectangular slot shaped DGS etched at same location for comprehensively analyzing the performances is another major aim of the research. Further it concerns in the novel approach to comparatively analyze the effect in performances when the dimensions of the DGS were varied. The literatures on MPA design have explored lots of aspects related to design and optimization but this research investigated on a novel approach to design MPA operating at 5.9GHz, and comparatively analyzed the two different DGS techniques, hence presenting best performances, as a result the designed patch antenna is perfectly matched tuning at the reflection coefficient of -36.16 dB, the antenna resonates at 5.9 GHz and enhance the bandwidth up to 300 MHz. This paper in addition aims to investigate on comprehensive operation of conventional (based on calculation), Optimized (using Ansoft HFSS), and DGS (DB and rectangular Slot shape) configurations etched at the center of ground plain, so that it could serve as a foundation to address the inherent limitation and challenges included in the design of such inset feed MPA working at 5.9GHz band. Mathematical calculations, simulation setup, optimization techniques, antenna design procedure and performance measurements are described in depth in the design and analysis section.

Our research contributes, in the broader area of knowledge on nset-feed MPA designed with integrating a dumbbell (DB) type and slot type DGS, their performances were comparatively studied. By fabricating the mentioned DGS the antenna was implemented at 5.9 GHz frequency, so that it could contribute to the reuse of the surplus unlicensed band of

ubiquitous RF energy. Based on rigorous simulations and measurements, the results reported in this research offer a thorough knowledge of the benefits and drawbacks of the suggested designs. The results of this study may guide future advancements in wireless communication systems, where small and effective antennas are essential, as we negotiate the complexities of antenna design.

## 2. ANTENNA DESIGN AND PERFORMANCE ANALYSIS

The geometry of the proposed inset feed micro-strip patch antenna along with the detail calculation for FR 4 substrate using general design equations [4], [12]. The design of the antenna includes a few pairs of stages; in the primary stage, the micro-strip patch antenna is designed for 50Ω impedance, and the secondary stage of design follows the optimizations for the width of the micro-strip feed ($w_f$) and inset notch gap (g) to tune the antenna at the desired resonant frequency. The defected ground structures (DGS) are etched on the ground surface for proper matching of impedance. The parametric variables are adjusted using the simulation software Ansys HFSS (High-Frequency Structure Simulator), which is based on the finite element approach, to achieve the intended performance of the constructed antenna.

### 2.1 Conventional Inset Feed Antenna Calculation and Modeling

The schematic diagram of initially proposed conventional type inset-feed MPA that resonates at 5.9 GHz frequency along with the detail dimensions is shown in Figure 1. The proposed antenna is designed on a glass epoxy substrate (FR4) with a relative permittivity (Γ) of 4.4, a loss tangent value of 0.02, and a thickness of 1.6 mm.

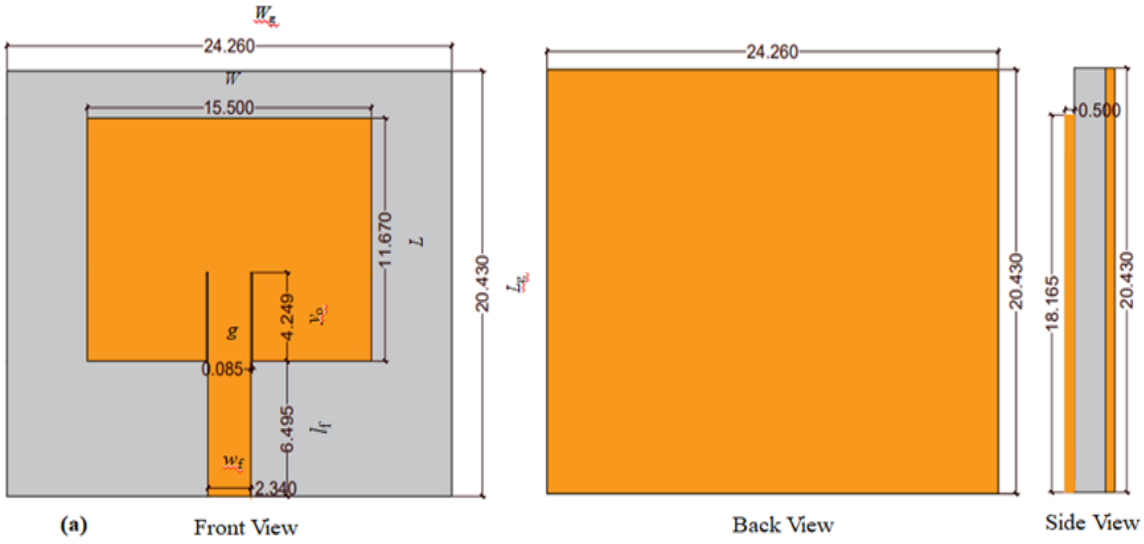


**Figure 1:** Schematic diagram of initially proposed conventional inset-feed MPA that resonates at 5.9 GHz frequency

The antenna dimensions based on the operating frequency ($f_r$) of interest were computed using the approximated equations deducted by implementing the concept of transmission model analysis [4], [7], [9], [12], [13].

The width of the patch (w) is given by

$$w = \frac{c}{2f_r\sqrt{\frac{\varepsilon_r+1}{2}}} \tag{1}$$

The length of the patch (L) is given by

$$L = L_{eff} - 2\Delta \tag{2}$$

Where, $L_{eff} = \frac{c}{2f_r\sqrt{\varepsilon_{reff}}}$

and $\varepsilon_{reff} = \frac{\varepsilon_r+1}{2} + \frac{\varepsilon_r-1}{2}\left[1 + \frac{12h}{w}\right]^{-0.5}$ ; $\frac{w}{h} > 1$

and $\frac{\Delta L}{h} = 0.412\left[\frac{(\varepsilon_{reff}+0.3)\left(\frac{w}{h}+0.264\right)}{(\varepsilon_{reff}-0.258)\left(\frac{w}{h}+0.8\right)}\right]$

Where, $\varepsilon_{\text{reff}}$, $L_{eff}$ and $c$ are effective dielectric constant, effective length, and free space velocity ($3\times10^8$ m/s) respectively.

The width ($w_g$) and length ($L_g$) of the ground plane were approximated using the concept as stated in the equations (3) and (4) [6].

$$L_g = L + 6h \tag{3}$$

$$w_g = w + 6h \tag{4}$$

Where, symbols have the usual meaning as explained above.

**2.2 Feed Calculation**

The antenna, which typically has a 50 Ω impedance to match a 50 Ω micro-strip line, is designed using micro strip line analysis. Because of this, the employed micro-strip line and antenna have a great match. Therefore, computing the feed line and the inset feed dimensions of the antenna is very important. So, feed length, feed width, inset depth, and notch gap are computed using the equations (5) – (8) [6], [9], [12].

The feed length is given by

$$l_f = \frac{\lambda_g}{4} \tag{5}$$

Where, $\lambda_g = \frac{\lambda}{\sqrt{\varepsilon_{reff}}}$

The feed width is given by

$$w_f = h.\frac{e^A}{e^{2A}-2} \tag{6}$$

Where, $A = \frac{z_0}{60}\sqrt{\frac{\varepsilon_r+1}{2}} + \frac{\varepsilon_r+1}{\varepsilon_r-1}(0.23 + \frac{0.11}{\varepsilon_r})$;

For $z_0 = 50\ \Omega$

An inset depth or length is given by

$$y_0 = \frac{L}{\pi} cos^{-1}\left(\sqrt{\frac{z_0}{z_{in}}}\right) \tag{7}$$

Where, antenna radiation impedance,

$$z_{in} = 90\left(\frac{\varepsilon_r^2}{\varepsilon_r - 1}\right)\left[\frac{L}{w}\right]^2$$

The feed gap or notch gap is given by

$$g = \frac{c}{\sqrt{2\,\varepsilon_{reff}}}\left(\frac{4.65\times10^{-12}}{f_r\,(GHz)}\right) \tag{8}$$

Using the equations (1) - (8) various antenna parameters were calculated, which are presented in the Table 1 as conventional values. Further the few parameters are optimized in order to tune the antenna at desired frequency.

**Table 1**: The geometrical parameters of the proposed inset feed patch antenna (unit: mm)

| Parameters | $L_g$ | $w_g$ | $L$ | $w$ | $l_f$ | $w_f$ | $y_0$ | $g$ |
|---|---|---|---|---|---|---|---|---|
| Conventional values | 20.43 | 24.26 | 11.67 | 15.5 | 6.495 | 2.34 | 4.249 | 0.085 |
| Optimized values | 24.66 | 24.66 | 11.67 | 15.5 | 6.495 | 3 | 4.249 | 0.3 |

Theoretically, antenna with full ground plane resonates at half-wavelength. The resonating frequency ($f_r$) is computed using the formula in equation (9) [12].

$$f_r = \frac{c}{\lambda_g \sqrt{\varepsilon_{reff}}} \tag{9}$$

Here, $\lambda_g$ is the guided wavelength at desired frequency.

To attain the impedance matching performance at the desired frequency (i.e., 5.9 GHz) along with enhanced bandwidth, the conventionally computed antenna radiator was modified for its inset notch gap and width of micro-strip line. The S-parameter plot of different antenna configurations is shown in Figure 2, which shows the return loss (S11) adversely increased to -30.2 dB from the conventional S11 magnitude of -16.59 dB after optimization. The slight increment in the resonant frequency towards the desired frequency value is also noticed during this time. Further, the initial metallic ground plane was modified by subtracting a dumbbell-shaped DGS and a rectangular slot-shaped DGS from the central location of the ground plane. More promising impedance-matched performances were obtained, resonate the antenna at 5.85 GHz corresponding to -36.16 dB of return loss within the impedance bandwidth range of 5.6768 GHz to 5.9798 GHz for the DGS DB configuration. Similar performances were noticed for the DGS with a rectangular slot configuration. The simulated S-parameter values for the different configurations of proposed antenna are comparatively plotted in Figure 2.

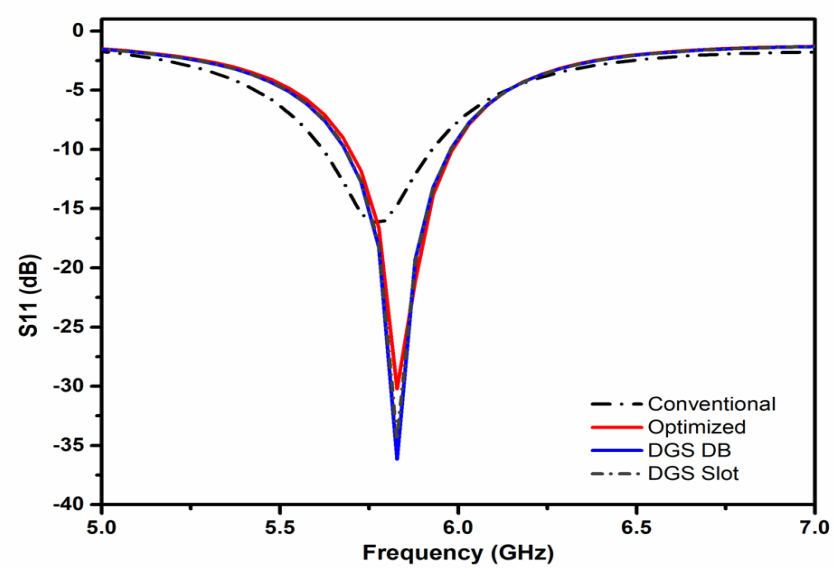


**Figure 2:** The return loss (S11) plot of different antenna configurations

### 2.3 Etching DGS: Dumbbell and Rectangular Slot

The dumbbell-shaped DGS (DB) and rectangular slot type DGS were etched and embedded at the center of the ground plane of the microwave circuit, as depicted in Figure 1. Integrating DGS in the ground plane will interrupt the surface current distribution. Introducing DGS modifies the properties like resistance, capacitance, and inductance of the ground plane; hence, any defects etched on the ground surface alter the effective capacitance and inductance of the ground by adding resistance, capacitance, and inductance [5], [14],[15]. It is easy to fabricate and intends to reduce the size of the antenna with an easily realizable, compact equivalent electrical circuit.

The applicability of the DGS unit is that the S-parameters obtained by simulation can be realized in the one-pole Butterworth low-pass response. The effective series inductance rises with increasing unit lattice etched area, and as the series inductance rises, the cutoff frequency decreases. The attenuation pole position shifts up to a higher frequency as the effective

capacitance decreases with increasing etched gap distance. Hence, the equivalent circuit parameters are computed as the DGS and Butterworth low-pass filters' reactance levels are equivalent at the cutoff frequency to match each other [16].

### 2.4 Performance analysis of DGS

#### *2.4.1 Dumbbell effect*

The length and width of the two rectangles of the dumbbell DGS unit cell and a connecting slot are the major parameters that affect the performance of the antenna. Improvements of bandwidth, reflection coefficient, along with proper matching of impedance are the major advantages of DGS unit cells. Here, a dumbbell-shaped defected area with two rectangles of size (a × b) = (0.5mm × 0.5mm) and a connecting gap of size (x × y) = (0.4mm × 2mm) is etched at the center of the backside metallic ground plane of the antenna.

The rectangular components of the dumbbell DGS increases the current path by changing the micro-strip line's effective inductance and capacitance. The capacitive impact of the dumbbell DGS is added by the two rectangular slots, and the addition of the inductance to the overall impedance are made up of the thin rectangular defective slot that links the two rectangular shaped flaws. Effective capacitance and effective inductance are inversely correlated with the slotted area of the DGS. A decrease in cut-off frequency is produced by increasing the slotted DGS area since it increases the effective inductance. The reduction in DGS area lowers the effective capacitance, which raises the resonant frequency [14]. This phenomenon can be clearly viewed from the S11 plot of the DGS effect for different values of dumbbell rectangles as shown in Figure3.

By altering the width (a) and length (b) of the two DGS in the ground plane, as well as the width of the slot (x) connecting the two DGS, a parametric analysis was carried out to determine the best values for the length and breadth of the DB DGS to tune at the lowest possible reflection coefficient. This demonstrated how the DGS affected the antenna's performance. Figure 3 displays the antenna's return loss for various values of a, b, and x.

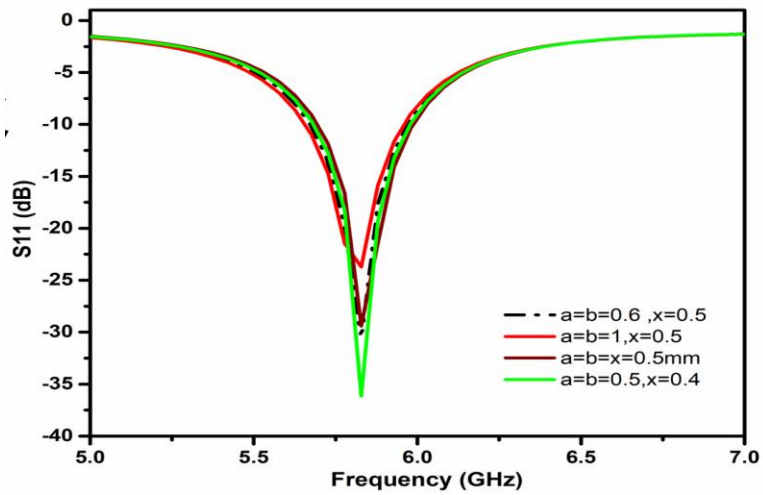


**Figure 3:** DB-shaped DGS effect analysis in S11 of antenna for different values of dumbbell dimensions

The DB DGS performance was optimized at a=b=0.5mm and x=0.4mm, where it gives a proper matching performance at a superior value of return loss (S11) of -36.16. It is visualized that by reducing the area of rectangles in DGS, the resonating frequency was slightly shifted towards a higher value along with the gradual decrement in the return loss, which indicates the proper matching of impedance. Also, there is a slight increment in the operating bandwidth of the antenna.

### *2.4.2 Slot Effect*

To analyze the effect of different structures, an optimized rectangular slot of size (width a = 0.51 and length b = 3.02) was also etched. As explained by the DGS DB working principle, a rectangular slot also holds a similar basic concept, so integrating slot-type DGS in the ground plane will interrupt the surface current distribution. Introducing slot DGS modifies the properties like resistance, capacitance, and inductance of the ground plane; hence, any defects etched on the ground surface alter the effective capacitance and inductance of the ground by adding resistance, capacitance, and inductance [5] [14,15]. It is easy to fabricate and intends to reduce the size of the antenna with an easily realizable, compact equivalent electrical circuit. An additional inductance is produced by the magnetic flux flow in the etched-out aperture and ground-plain gap capacitance as a result of the insertion of the rectangular slot defect on the ground plain. An etched flaw alters the surface impedance; this therefore influences the shield current's distribution over the plain.

The current's phase velocity is changed by the variation in surface impedance. The apparent effective permittivity varies as a result of the phase velocity shift. Because of the flaw created on the ground plane, we can see that the surface current is distributed evenly, increasing the fringing field [7], [15].

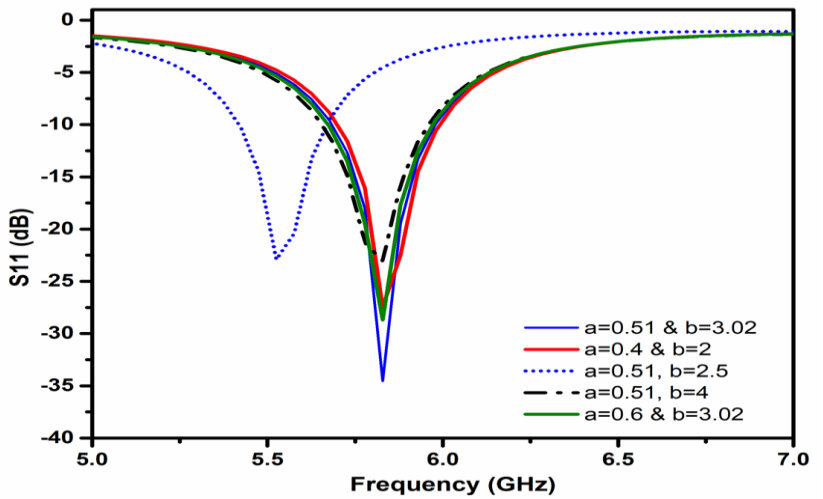

**Figure 4:** DGS affect analysis in the S11 of the antenna when varying the dimensions of the rectangular slot.

As plotted in Figure 4 represents the effect of varying dimensions of Slot type DGS in the return loss and perfect tuning of the antenna towards the desired frequency, It is visualized that by increasing the length of the rectangular slot, the resonating frequency was slightly shifted towards a higher value along with the gradual decrement in the return loss finally tuning at -32.98 dB, at which the proper matching of impedance was obtained. Also, there is a huge increment in the operating bandwidth of the antenna compared to similar types of patch antenna reported in [7], [17].

## 3. RESULTS AND DISCUSSION

The rectangular micro-strip patch antenna was simulated and fabricated using FR4 glass epoxy material having a dielectric constant of 4.4 whose resonance frequency was set at 5.9 GHz, the Wi-Fi band. After that, a DGS in a dumbbell shape and a rectangular slot are integrated into the ground plane, and the simulations are run using ANSYS HFSS, which gives a solution for electromagnetic structures using the finite element method. Data analysis was performed using Origin software. The inset feeds micro-strip patch antenna inbuilt with both dumbbell DGS and slot DGS was fabricated, investigated, and characterized using the Vector Network Analyzer (VNA). Then a comparative analysis was performed with the conventional antenna.

### 3.1 Scattering Parameter

The simulated and measured reflection coefficients (S11) of the inset feed patch antenna etched with DB DGS and Slot DGS on the ground plane were plotted. A comparison of the simulation and measurement results is seen in the plot in Figure 5, which indicates that both types of proposed printed configurations indicate the same impedance bandwidth of 300 MHz with a good return loss value, which shows good agreement with the impedance bandwidth seen in the simulation. Although a very small shift in the resonance frequency was noticed beyond the desired frequency, the frequency of resonance was still within the impedance bandwidth. Such faults in the prototype are created due to the imperfection in the fabrication and soldering of the antenna. The printed prototype covers the matching band (i.e., S11 = -10 dB) ranging between 5.833 and 6.132 GHz.

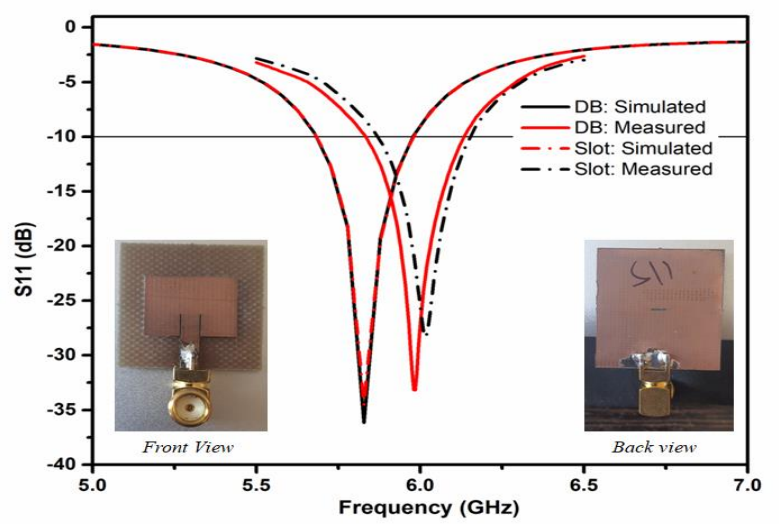


**Figure 5:** Comparisons of the simulated and measured return loss of the proposed antenna and Image of the printed prototype

### 3.2 VSWR (Voltage Standing Wave Ratio) and Impedance

A positive real number signifies effective impedance matching between the feed line and the antenna [18]. The VSWR (Simulated value of 1.03 and measured value of 1.05 for DB

DGS) and impedance plot as depicted in Figure 6 for the proposed antenna indicate that both are efficiently transmitting the radio frequency with perfect impedance matching, so the VSWR and impedance plots of the antenna are analyzed together. Further, the impedance plot significantly reflects there is a gradual improvement towards 50Ω impedance matching from the conventional design to optimized and then with DB-shaped DGS. Printed prototype etched with DB-shaped DGS exhibits even accurate impedance matching tuning at the desired frequency. VSWR is expressed in terms of the reflection coefficient (Γ), which depends on the load impedance ($Z_L$) and the characteristic impedance ($Z_0$).

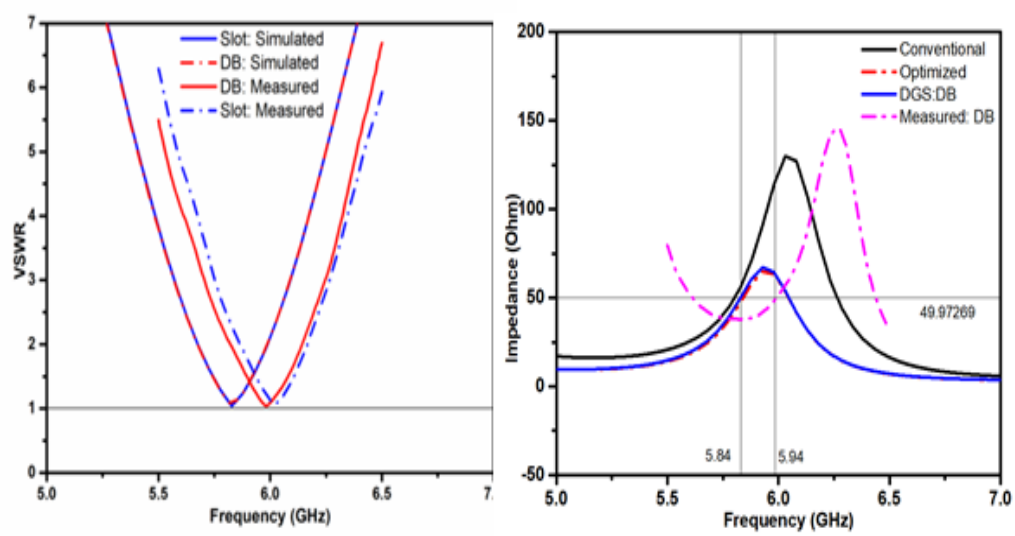


**Figure 6:** Comparative plot of VSWR and impedances obtained for simulated value and measured value

### 3.3 Antenna Radiation Characteristics and Gain

The 2D and 3D radiation patterns of the designed antenna obtained at 5.9 GHz are plotted in Figure 7. The antenna exhibited a unidirectional radiation pattern in the E-plane ($\varphi = 0^0$), where a maximum power of 4.72 dB was transmitted. From the surface current image of

the antenna in Figure 8, it was observed that the maximum current distribution concentrated towards the edges of the patch through the surface. At higher frequencies, a skin effect occurs, due to which current flows through the edges instead of the central region of the conductor. On the ground plane, current distribution was observed surrounding the DGS with a similar wave pattern, creating unipolar radiation.

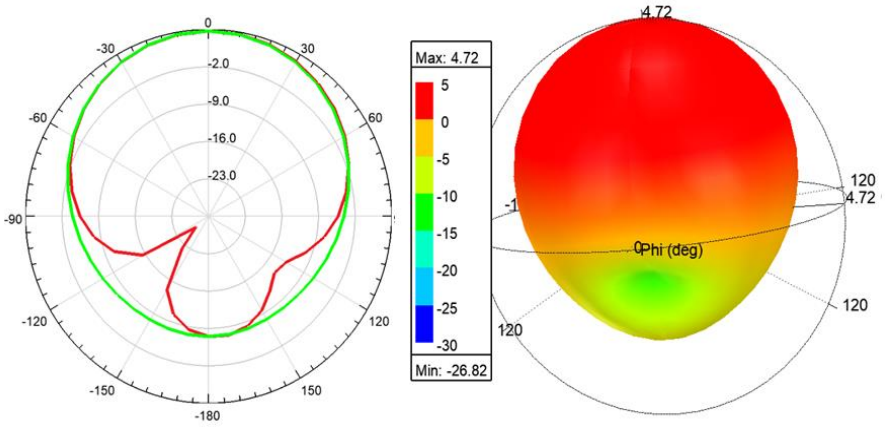


**Figure 7:** 2D and 3D radiation pattern of the proposed antenna (MPA etched with DB-shaped DGS)

The radiation efficiency of the antenna was observed at 70% at 5.9 GHz. The measured gain and the simulated gain at the corresponding resonance frequency are comparatively plotted in Figure 9, which justifies a good match between the simulated value and the measured value for the developed prototype of the proposed antenna.

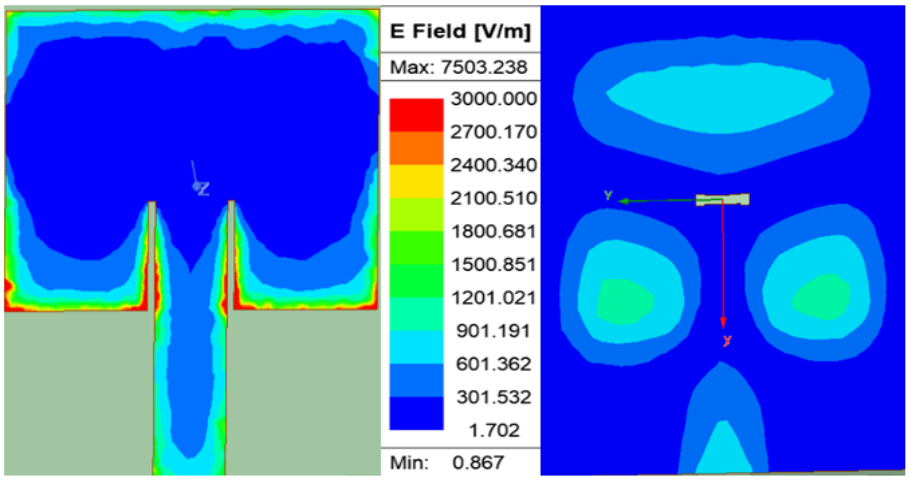


**Figure 8:** Surface current of the antenna (etched with DB DGS) at 5.9 GHz

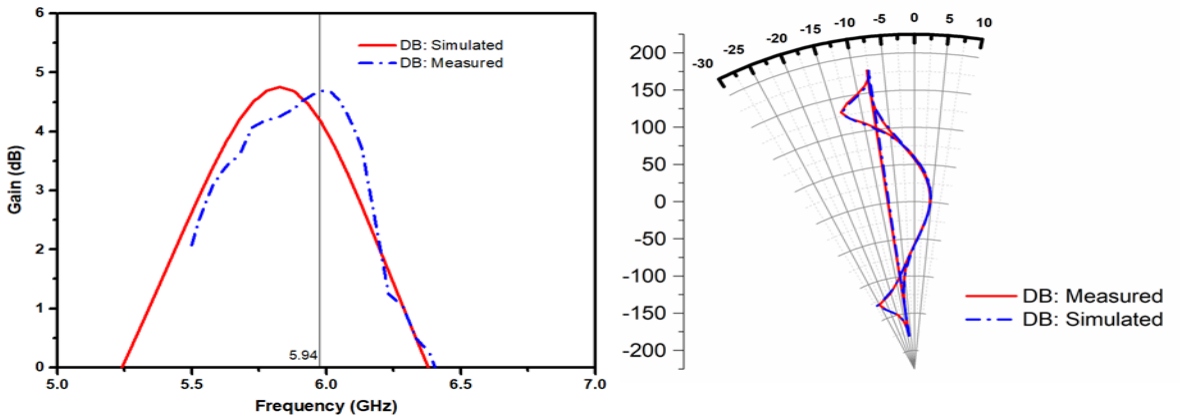


**Figure 9:** Gain plot of the proposed antenna concerning the frequency and the beta

**Table 2:** Antenna performance parameters analysis of simulated antenna with various configurations and printed prototype antenna etched with DB-shaped DGS.

| **Antenna Configurations** | **Bandwidth (MHz)** | **Return Loss (dB)** | **VSWR** | **Gain (dB)** | $f_r$ **(GHz)** |
|---|---|---|---|---|---|
| Conventional | 257 | -16.59 | 1.44 | 4.78 | 5.75 |

| | | | | | |
|---|---|---|---|---|---|
| Optimized (Opt.) | 279.8 | -30.2 | 1.06 | 4.69 | 5.82 |
| Opt. + DGS: Slot | 303 | -32.98 | 1.04 | 4.73 | 5.84 |
| Opt. + DGS: DB | 303 | -36.16 | 1.03 | 4.72 | 5.84 |
| Printed DB (Measured) | 300 | -33.16 | 1.05 | 4.68 | 5.94 |

Table 2 presents the comparisons among the various antenna parameters for the different configurations of antenna like simulated data obtained from conventional (design based on calculations), optimized (using Ansoft HFSS), optimized antenna etched with rectangular slot and dumbbell (DB), and finally with the measured data of printed prototype (Optimized and etched with DB DGS, as best performances are obtained for it in simulation). The data presented in Table 2 declared that the printed prototype and the simulated proposed antenna have a very good match in their performances, with excellent S11, bandwidth, VSWR, and gain.

## 4. CONCLUSIONS

The antenna designed and fabricated in this research is an inset feed microstrip patch antenna based on DGS for Wi-Fi band application. The common patch-type geometry was implemented, utilizing the advantages of DGS to operate at 5.9 GHz. The slot type and DB type of DGS were etched, and we compared the simulated and measured data of each with the conventionally computed patch antenna. The performance of DB DGS tuning at a return loss

of -36.16 dB was found to be the best in all performances, so it was fabricated and a detailed analysis was further performed.

With a peak gain of 4.72 dB and a radiation efficiency of 70%, the designed antenna attained a measured impedance bandwidth (i.e., S11≤10 dB) of 300 MHz ranging between 5.833 GHz and 6.132 GHz. The suggested antenna with a perfectly matching impedance is suitable for Wi-Fi band communication at 5.9 GHz. The measurements of the prototype declared good agreement with the simulated results and hence showcased the significantly improved performance compared to similar patch antennas published earlier.

## CONFLICTS OF INTEREST

The authors declare no conflicts of interest.

## DATA AVAILABILITY STATEMENT

Not Applicable

## References

[1] Zhang, X., Grajal, J., Vazquez-Roy, J. L., Radhakrishna, U., Wang, X., Chern, W., Zhou, L., Lin, Y., Shen, P. C., Ji, X., Ling, X., Zubair, A., Zhang, Y., Wang, H., Dubey, M., Kong, J., Dresselhaus, M., & Palacios, T. (2019). Two-dimensional MoS2-enabled flexible rectenna for wi-fi band wireless energy harvesting. *Nature*, *566*(7744), 368–372. https://doi.org/10.1038/s41586-019-0892-1, PubMed: 30692651

[2] Tran, L.-G., Cha, H.-K., & Park, W.-T. (2017). RF power harvesting: A review on designing methodologies and applications. *Micro and Nano Systems Letters*, *5*, 1–16.

[3] Ibrahim, H. H., Singh, M. J., Al-Bawri, S. S., Ibrahim, S. K., Islam, M. T., Alzamil, A., & Islam, M. S. (2022). Radio frequency energy harvesting technologies: A comprehensive review on designing, methodologies, and potential applications. *Sensors*, *22*(11), 4144. https://doi.org/10.3390/s22114144

[4] Hussain, M., Mousa Ali, E., Jarchavi, S. M. R., Zaidi, A., Najam, A. I., Alotaibi, A. A., Althobaiti, A., & Ghoneim, S. S. M. (2022). Design and characterization of compact broadband antenna and its MIMO configuration for 28-GHz 5-G applications. *Electronics*, *11*(4), 523. https://doi.org/10.3390/electronics11040523

[5] Rahman, M. M., Islam, M. S., Wong, H. Y., Alam, T., & Islam, M. T. (2019). Performance analysis of a defected ground-structured antenna loaded with stub-slot for 5-G communication. *Sensors*, *19*(11), 2634. https://doi.org/10.3390/s19112634

[6] Rambe, A. H. et al. (2020), "Design and simulation of rectangular patch micro-strip antenna with inset feed for S-band application," In *IOP Conference Series*. *Materials science and engineering*. IOP Publishing.

[7] Anita, R., & Kumar, C. (2015). Analysis of microstrip antenna performance by varying length of rectangular slot DGS. In International Conference on Emerging Research in Electronics, Computer Science and Technology (ICERECT), *2015*. IEEE Publications. https://doi.org/10.1109/ERECT.2015.7498984

[8] Chin, C. K., Awang Mat, D. A., Truna, M. N., Abg Zaidel, D. N., Kanaya, H., Sahrani, S., anak Hong Ping, K., Kipli, K., & Joseph, Aa. (2020). Design of dumbbell shaped DGS-Notch patch antenna for microwave imaging system. *International Journal of Integrated Engineering*, *12*(6), 94–104. https://doi.org/10.30880/ijie.2020.12.06.012

[9] Awan, W. A., Naqvi, S. I., Naqvi, A. H., Abbas, S. M., Zaidi, A., & Hussain, N. (2021). Design and characterization of wideband printed antenna based on DGS for 28-GHz 5-G applications. *Journal of Electromagnetic Engineering and Science*, *21*(3), 177–183. https://doi.org/10.26866/jees.2021.3.r.24

[10] Sandi, E., Rusmono, R., Diamah, A., & Vinda, K. (2020). Ultra-wideband microstrip array antenna for 5-G millimeter-wave applications. *Journal of Communications*, *15*(2), 198–204. https://doi.org/10.12720/jcm.15.2.198-204

[11] Hussain, M. B., Butt, M., Nadeem, Z., Zahid, M., & Amin, Y. Design of dual-band microstrip patch antenna for wireless local area network applications. *Engineering Proceedings*, *46*(1): 3, 2023. https://doi.org/10.3390/engproc2023046003

[12] Balanis, A. C. (January 2016). *Antenna theory: Analysis and design* (4th ed). John Wiley & Sons.

[13] Rajan, V., Prakash Karavilavadakkethil, C., Vinesh Puthiyapurayil, V., Pezholil, Mohanan, & Kesavath, V. (2021). Coplanar waveguide-fed electrically small via-less antenna for dual band applications. *IETE Journal of Research*. https://doi.org/10.1080/03772063.2021.1947906

[14] Mukesh Kumar, K., Binod Kumar, K., & Sachin, K.. (2017). Defected ground structure: Fundamentals, analysis, and applications in modern wireless trends. *International Journal of Antennas and Propagation*, *2017*, article ID 2018527, 22 pages. https://doi.org/10.1155/2017/2018527

[15] Roy, S. M., Karmakar, N. C., & Balbin, I.. (2007) Dumbbell-shaped defected ground structure. *International Journal of RF and Microwave Computer-Aided Engineering*, 17(2), 210–224. https://doi.org/10.1002/mmce.20215

[16] Weng, L. H., Guo, Y.-C., Shi, X.-W., & Chen, X. (2008). An overview on defected ground structure. *Progress in Electromagnetics Research B*, *7*, 173–189. https://doi.org/10.2528/PIERB08031401. http://www.jpier.org/PIERB/pier.php?paper=08031401

[17] Abdul Hussein, Alaa and Hassan, Ali and Naser, Ahmed., Design and implementation of microstrip patch antenna using inset feed technique for 2.4 GHz applications, (2021). *International Journal of Microwave and Optical Technology*, *16*, 355–361.

[18] Best, S. R., Altshuler, E. E., Yaghjian, A. D., McGinthy, J. M., & O'Donnell, T. H. (2008). An impedance-matched 2-element super directive array. *IEEE Antennas and Wireless Propagation Letters*, *7*, 302–305. https://doi.org/10.1109/LAWP.2008.921372